Title

Integrin-driven actin polymerization consolidates long-term potentiation.

Permalink

https://escholarship.org/uc/item/9x03k4z9

Journal

Proceedings of the National Academy of Sciences of the United States of America, 103(14)

ISSN

0027-8424

Authors

Kramár, Enikö A
Lin, Bin
Rex, Christopher S
<u>et al.</u>

Publication Date

2006-04-04

Peer reviewed

Integrin-driven actin polymerization consolidates long-term potentiation

Enikö A. Kramár*, Bin Lin*, Christopher S. Rex†, Christine M. Gall†‡§, and Gary Lynch*

Departments of *Psychiatry and Human Behavior, ‡Anatomy and Neurobiology, and †Neurobiology and Behavior, University of California, Irvine, CA 92697

Long-term potentiation (LTP), like memory, becomes progressively more resistant to disruption with time after its formation. Here we show that threshold conditions for inducing LTP cause a rapid, long-lasting increase in polymerized filamentous actin in dendritic spines of adult hippocampus. Two independent manipulations that reverse LTP disrupted this effect when applied shortly after induction but not 30 min later. Function-blocking antibodies to $\beta 1$ family integrins selectively eliminated both actin polymerization and stabilization of LTP. We propose that the initial stages of consolidation involve integrin-driven events common to cells engaged in activities that require rapid morphological changes.

adenosine | consolidation | hippocampus | spines | theta burst

That newly formed memories are vulnerable to disruption was clearly articulated by Ribot (1) in the late 19th century and was probably common knowledge long before that. Systematic analysis of this phenomenon in animals (2) established that stabilization (or consolidation) begins 30–60 sec after learning and progresses over the next 30–60 min. Additional work uncovered stages of consolidation that were delayed by hours or even days (3, 4). Although much evidence indicates that protein synthesis is required for the later phases of consolidation (5, 6), the nature of events that stabilize memory in the first few minutes after learning remains unknown. However, recent developments in the study of long-term potentiation (LTP), a form of synaptic plasticity widely accepted as a substrate of commonplace memory, have begun to describe a possible mechanism for the rapid phase of consolidation. Specifically, induction of LTP in adult hippocampus with naturalistic theta-pattern stimulation causes pronounced increases in filamentous (F)-actin in individual spines within the dendritic regions containing potentiated synapses (7). Local cytoskeletal reorganization, as indicated by these results, would be expected to cause persistent modifications to the structure, and thus function, of synapses.

The present studies addressed two essential features of the above summarized cytoskeletal hypothesis for the rapid phase of consolidation. First, is spine actin polymerization actually responsible for the stabilization of LTP? Like memory, LTP passes through multiple "consolidation" periods (8, 9), including an initial 30-min episode after theta stimulation (10, 11). We tested whether manipulations known to disrupt LTP shortly after its induction also reverse actin polymerization and whether these treatments become ineffective once potentiation is stabilized. Additional experiments were run to test whether, as necessarily predicted by the hypothesis, the threshold for inducing stable LTP corresponds with that for increasing F-actin levels in spines. Second, what is the process that converts intense afferent activity into actin polymerization? Matrix adhesion receptors belonging to the integrin family regulate the actin cytoskeleton across many cell systems, including developing neurons (12), and are potential triggering agents for the F-actin effects produced by theta stimulation. Moreover, integrin ligands, neutralizing antibodies, and partial knockouts (13–17), as well as inhibitors of integrin-associated tyrosine kinases (18, 19), selectively block LTP consolidation. Here we used selective antagonists to test the specific prediction that $\beta 1$ integrins are responsible for the spine actin changes that accompany LTP.

Results

Rhodamine-phalloidin was used to label F-actin. In contrast to its typical use in studies of neuronal cytoskeleton, we have found that the label can be applied to living cells and then visualized after fixation. Initial experiments with this procedure used intracellular diffusion from whole-cell recording electrodes, but subsequent work described conditions under which extracellular treatment was fully effective (7). With this approach, there is very little background staining and only faint in situ labeling of spines in control tissue, making it possible to visualize densely labeled spines and dendritic segments in the complex three-dimensional environment of adult hippocampus. Fig. 1 illustrates these points and describes the techniques used to count spines. Shown are sections through slices that received control or theta-burst stimulation (TBS) (Fig. 1 Ai and Aii); pseudocolor images showing the fluorescence intensity are presented below these two micrographs (Fig. 1 Aiii and Aiv). Computerized counting was done of all profiles with pixel intensity above a threshold value established for each experiment (note the color bar in Fig. 1Aiv) and physical dimensions (area and diameter) that fall within the range expected for spines (10). Fig. 1Av illustrates the profiles counted by the program for the theta-burst case. Numerical comparisons of the number of spines and mean relative pixel intensity for the two groups of slices are summarized in Fig. 1B.

We first tested whether actin polymerization is triggered by conditions that are at or above stimulation threshold for producing stable potentiation; 2 (below LTP threshold), 5 (above threshold), or 10 (typical train) theta-burst stimuli were delivered to the Schaffer commissural afferents to CA1b stratum radiatum in the presence of locally applied rhodamine-phalloidin (see Fig. 2A for physiological results). The micrographs in Fig. 2B show that labeled profiles were infrequent in the 2-burst group but numerous in the 5- and 10-burst cases. The rhodamine-positive structures in groups receiving 5 and 10 theta bursts corresponded in size to spine heads and were connected by thin necks to faintly labeled dendritic branches (Fig. 2B Inset). Notably, increases only occurred in stratum radiatum, that lamina containing the stimulated afferents. Quantification of labeled profiles from blind counting with an automated system is summarized in Fig. 2C; 5 and 10 bursts produced a 10-fold increase in phalloidin-labeled spines, whereas the 2-burst group did not significantly differ from control slices ($P = 0.20$, two-tailed t test; same statistic used throughout the text).
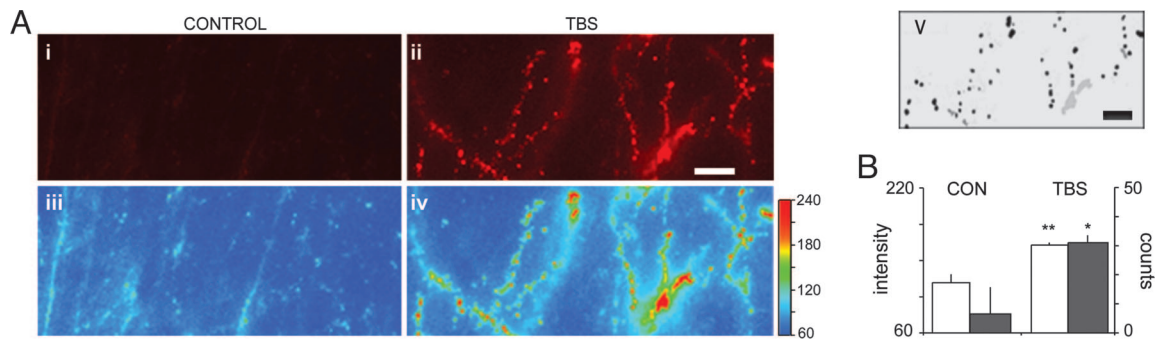
These findings were confirmed by using labeling obtained with phalloidin infusion through whole-cell recording electrodes. Cell bodies and proximal dendrites are routinely labeled with this

NEUROSCIENCE

Fig. 1. TBS produces increased phalloidin-label intensity in spines. (*A*) Photomicrographs of *in situ* rhodamine-phalloidin-labeled hippocampal slices stimulated either with continuous baseline stimulation (control) (*i*) or with TBS (*ii*). Pseudocolor images (*iii* and *iv* for control and TBS, respectively) were generated by cropping the image-intensity range from poorly illuminated to maximally bright profiles and then assigning intensity values (pixel intensity units, PIUs) to a rainbow scale (*iv Right*) from blue/lowest to red/highest relative fluorescence. (Scale bar in *ii*, 10 μm.) Output of spine-counting algorithm (*v*, bottom right) for image in *ii*: Intensity threshold was set at 160 PIUs (compare with color calibration) to discriminate between brightly and faintly labeled spine-like structures. Counted spines are labeled in black, and all other noncounted entities with intensities above threshold are labeled in gray. (Scale bar in *v*, 10 μm.) (*B*) Bar graph plots the average relative spine intensity (left *y* axis; open bars) of counted spines in control vs. TBS-treated slices. Average relative spine intensities were greater in TBS-treated slices (*n* = 5) compared with controls (*n* = 5; **, *P* = 0.005, two-tailed *t* test). Plotted against a second *y* axis (right; filled bars) is the number of spine observations counted by the algorithm (*Av*) in these same slices with pixel intensity threshold set to 160 PIUs (*, *P* < 0.01). CON, control.

technique, but stained secondary branches and spines are rare in control slices (Fig. 2*D*). Labeled spine heads in cells receiving five theta bursts were 5-fold greater in number than those receiving two bursts (*P* = 0.009). In all, the stimulation threshold for activity-induced actin polymerization in the adult hippocampus was close to that for producing stable LTP.

We next tested whether actin polymerization can be disrupted before the completion of consolidation. LTP is vulnerable to a number of treatments, including low-frequency stimulation (11, 20–22) and adenosine A1 agonists (23) during the 30- to 60-min consolidation period. We tested the effects of each of these manipulations on theta-induced increases in spine actin labeling. Stimulation of Schaffer collateral afferents to CA1 stratum radiatum with 10 theta bursts reliably induced stable potentiation. Fig. 3*A* shows that a 1-min train of 5-Hz stimulation applied 30 sec after the bursts completely blocked the formation of LTP. Labeled spines were almost totally absent in these cases, whereas they were prominent in slices expressing LTP (Fig. 3*B*). Importantly, the loss of F-actin-dense spines was reproduced when the delay between theta bursts and low-frequency stimulation was increased to 2 min, a time point at which increases in labeling are fully developed (10); it thus appears that the postinduction stimulation reverses, as opposed to prevents, polymerization. Quantitative analyses confirmed these points (Fig. 3*C*). Stimulation of adenosine A1 receptors also eliminates recently formed LTP (23) and mediates the time-dependent reversal effect obtained with low-frequency stimulation (20, 22). Adenosine proved to be potent in blocking theta-burst-induced actin polymerization when applied immediately after TBS (Fig. 3*D*). The difference in spine labeling between the TBS-alone vs. TBS-plus-adenosine treatment groups was significant (*P* = 0.004).

Whatever its cellular nature, it is clear that LTP consolidation renders potentiation progressively more resistant to disruption with time after stimulation. We next asked whether this temporal dependency also holds for polymerization of spine actin. One-minute trains of 5-Hz stimulation were delivered 30 min after TBS, a time point at which they do not reverse LTP. In marked contrast to their effects when delivered immediately after theta trains, the low-frequency stimulation applied 30 min after TBS had no effect on phalloidin labeling (Fig. 3*C*); there were 31 ± 3.7 (mean ± SD) labeled spines per 550 μm^2 in the TBS-alone group and 32 ± 8.1 in the experimental slices (*n* = 5 per group). These results point to the conclusion that recently formed

F-actin becomes gradually stabilized over the same period that LTP consolidates.

Rapid actin polymerization in many circumstances is initiated by integrins (12), and we tested whether this holds for LTP as well. The majority of integrins expressed in brain contain a β1 subunit (24), and it is known that multiple β1 family integrins are expressed in hippocampal field CA1, at least some of which are concentrated in synapses (3). Therefore, to test for integrin involvement in stimulation-induced increases in F-actin, function-blocking antisera to β1 integrin were topically applied to slices for 10 min before and after TBS. As shown in Fig. 4*A* and *B*, treatment with anti-β1 (MAB1987Z) effectively blocked LTP consolidation, whereas control serum had no effect on potentiation. The β1 antisera, but not control Ig, reduced spine labeling after TBS to a level comparable with that found in control slices (Fig. 4 *C* and *D*). Effects on spine labeling were replicated with a second antibody to β1 integrin (#555002) (data not shown).

Discussion

Integrin-initiated actin polymerization in various cell types can lead to morphological changes of considerable persistence as, for example, in anchoring migrating cells to final locations (25). Thus, it is not entirely unexpected that the integrin/actin system would be central to the production of LTP, a phenomenon that involves anatomical modifications (26–28) and has extreme duration as one of its defining characteristics (29, 30). Suppression of integrin functioning by various routes blocks LTP (13–15, 17, 31), as do agents that interfere with actin polymerization (32, 33). Moreover, intense afferent activity modifies the actin network within individual spines of neurons in dissociated cell culture (34, 35), organotypic cultures (36), and, most pertinent to the age-dependent LTP consolidation effect (37), slices from adult animals (7). The present studies asked whether integrin-driven changes in spine actin polymerization can account for the rapid phase of LTP and, by inference, memory consolidation. This prediction would require that the changes occur quickly, have a threshold comparable with that for the production of stable LTP, be vulnerable to disruption for several minutes, and then, after 30–60 min, become resistant to further manipulation. The hypothesis also requires that disruptions to appropriate integrins eliminate the effects of theta bursts on spine F-actin.

Each of the above predictions was tested and confirmed. Using intracellular and extracellular applications of rhodamine-
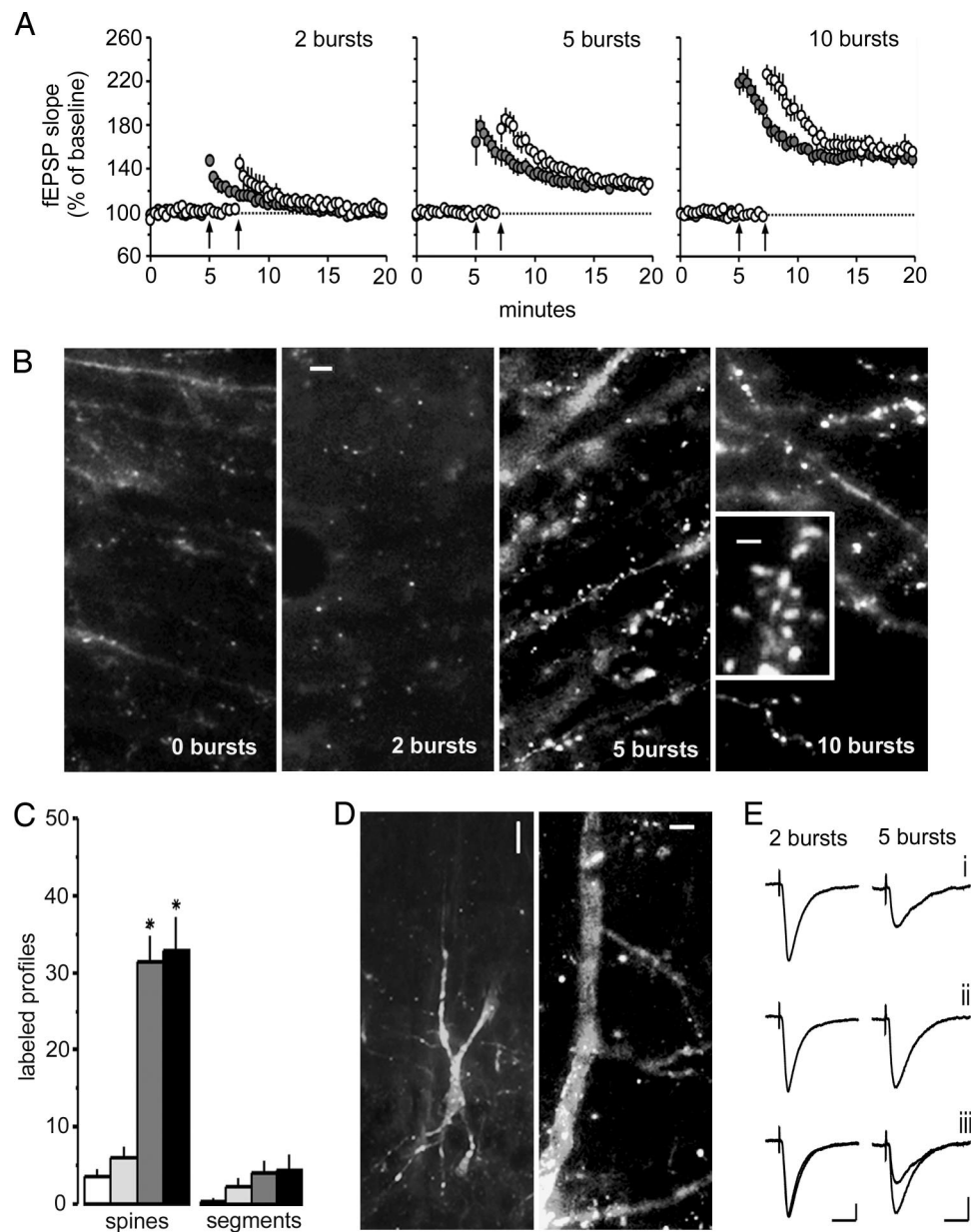
Fig. 2. Threshold for activity-induced actin polymerization corresponds to that for LTP. (*A*) Theta bursts (arrows) delivered to Schaffer commissural projections to CA1b in hippocampal slices treated with rhodamine-phalloidin; shown are the mean (±SEM) changes in fEPSP slope. Two theta bursts did not induce LTP, whereas 5 or 10 bursts did (*n* = 5 per group). (*B*) Slices were collected at the end of the experiment, fixed in paraformaldehyde for 12–16 h, immersed in sucrose, and sectioned. Labeled profiles corresponding to spine heads were largely absent in control and 2-burst groups but were numerous in 5- and 10-burst cases. (Scale bars, 5 μm.) High-magnification micrograph (*Inset*) shows densely labeled spines attached to secondary dendrites by thin, poorly stained processes. (Scale bar, 1 μm.) (*C*) Mean number of labeled spines in the stimulated field was greater in slices expressing LTP (5 bursts, dark gray bars; 10 bursts, black bars) than in control slices (open bars) or 2-burst slices (light gray bars) (*, *P* < 0.01). The number of densely labeled dendritic branches was not statistically different from control for any experimental group. (*D Left*) Labeling from a control cell sampled with a whole-cell electrode containing rhodamine-phalloidin. (Scale bar, 20 μm.) (*D Right*) Labeling in apical dendrites after five theta bursts. (Scale bar, 5 μm.) There were substantially more spines in five-burst (21 ± 11.1; *n* = 6) than in two-burst (4.0 ± 2.1, *n* = 5, *P* = 0.009) cells. (*E*) Whole-cell recordings show that phalloidin-filled electrodes did not disturb basic synaptic physiology: before (*i*), after (*ii*), and superimposed (*iii*) theta bursts. (Calibration, 50 pA, 20 ms.)

phalloidin, we found that theta bursts markedly and rapidly increase the number of spine heads containing F-actin in adult hippocampus, with the threshold for the effect being close to that for LTP. Two independent manipulations that selectively disrupt LTP consolidation (5-Hz stimulation and adenosine) also blocked actin polymerization when applied shortly after theta stimulation but were without effect when administered 30 min later. Pertinent to these results is evidence that antagonists of actin polymerization disrupt stabilization when applied imme-

diately after LTP induction (32); it would be useful to determine whether this disruption still holds with longer post-theta delays. Finally, with regard to the proposed triggering mechanism, infusion of function-blocking antibodies against β1 integrins, several of which are present in hippocampal synapses (see ref. 3 for a review), caused a near complete suppression of both the theta-induced increase in spine labeling and LTP stabilization.

The above results suggest that the rapid phase of LTP consolidation reflects integrin-induced changes in the spine
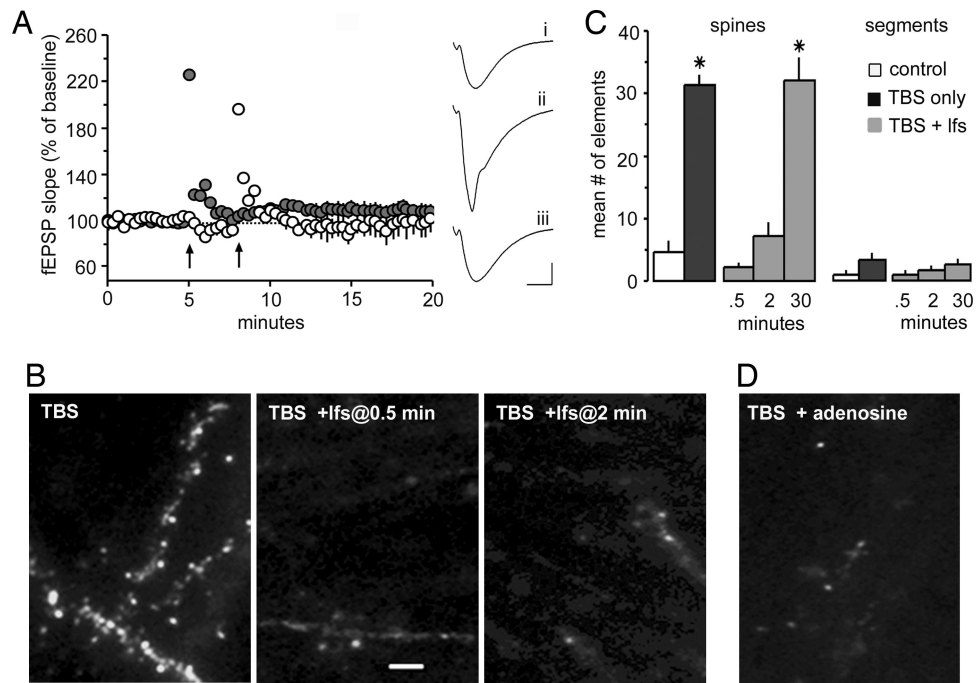
Fig. 3. Conditions that reverse LTP block actin polymerization. (*A*) Low-frequency stimulation (5 Hz, 1 min) delivered 30 sec after TBS (arrows) completely reverses LTP. The experiment was carried out on two collections of Schaffer commissural afferents (light and dark circles; *Left*) in each slice. (*Right*) Typical fEPSPs recorded before (*i*), 30 sec after (*ii*), and 30 min after (*iii*) TBS. (Calibration, 1 mV, 5 msec.) (*B*) Slices that received TBS (*n* = 5) or TBS followed by low-frequency stimulation (lfs) 30 sec (*n* = 5) or 2 min (*n* = 5) later were collected 15 min after TBS and processed for visualization of *in situ* labeling. (Scale bar, 5 μm.) Note the reduced number of labeled profiles in the cases that received lfs. (*C*) Mean number of labeled spines and dendritic segments in slices that received baseline stimulation (open bars), TBS (black bars), or TBS followed by lfs (TBS + lfs, gray bars). The low-frequency trains were delivered 0.5, 2, or 30 min after TBS. The number of labeled spines was lower in the 0.5- and 2-min groups relative to slices that had 30-min delays or that received TBS alone (*, *P* < 0.02; *t* tests); the number of profiles in the former two groups was not statistically different from controls (*P* > 0.5). The frequency of labeled dendritic segments did not differ between groups. (*D*) Adenosine (200 μM) infused immediately after TBS reduced the number of labeled spine heads (5.0 ± 2.6; *n* = 6) from that found with TBS alone (*P* = 0.007).

cytoskeleton that appear in <2 min and are stabilized over the next several minutes. The rapid appearance of high concentrations of F-actin in a subset of spines is consonant with work describing the 30-sec assembly of actin filaments in activated platelets (38). Studies with oocyte lysates using *in situ* labeling similarly show an increase in F-actin occurring in <50 sec (39). What could cause the observed stabilization of F-actin that occurs over the following several minutes? In many test systems, reorganization of the actin network by integrins is followed by attachment of crosslinking proteins, including spectrin, and anchoring of the assemblage to the membrane (12). Disassembly can occur in the absence of these latter steps. Spines and postsynaptic densities are enriched with spectrin (40) and related crosslinking/membrane attachment proteins [adducin (41), actinin (42), and others] and thus appear to have the components needed for local generation of stable modifications to the membrane cytoskeleton. Consolidation, according to the proposal being made here, involves processes comparable with those used by diverse cells to rapidly generate local structural modifications as occurs, for example, during migration.

There is significant overlap between the proteins and enzymes implicated in LTP and those with established roles in integrin-mediated regulation of the actin cytoskeleton (3). The present model, to the degree it is correct, thus somewhat simplifies the cell biology of the potentiation effect. However, the model's explanatory power is limited by the lack of any obvious link between the rapid mechanisms described above and the later, protein synthesis-dependent components of consolidation. There is evidence that theta stimulation causes the immediate proteolysis of key structural proteins (40, 43–46), an event that could both pave the way for a reorganization of the actin network

and create a need for newly synthesized proteins. In this regard, it will be of interest to test the nonintuitive prediction that protease inhibitors reported to block LTP will also prevent activity-induced increases in spine F-actin.

Finally, there is the essential question of whether the LTP stabilization mechanisms described here account for the initial phase of memory consolidation first described in detail more than 50 years ago (2). Although consolidation and dendritic spines are not necessarily involved, it is nonetheless of interest in this regard that pharmacological or genetic manipulations of actin chemistry disrupt learning (47–49). The *in situ* labeling procedure described in the present experiments may provide a way of directly testing whether learning episodes produce LTP-like changes to the actin network in discrete populations of spines in appropriately located brain regions. If so, then it would be possible to ask whether F-actin increases are reversed in a time-dependent manner by postlearning trial manipulations known to block memory consolidation.

Materials and Methods

Animals. Animal procedures were conducted in accordance with the National Institutes of Health *Guide for the Care and Use of Laboratory Animals* and with protocols approved by the Institutional Animal Care and Use Committee of the University of California at Irvine. Efforts were made to minimize animal suffering and numbers of rats used.

Hippocampal Slices and Extracellular Application of Rhodamine-Phalloidin. These studies used 350-μm-thick hippocampal slices (7, 14) prepared from young-adult (30- to 42-day-old) male Sprague–Dawley rats and maintained in an interface recording
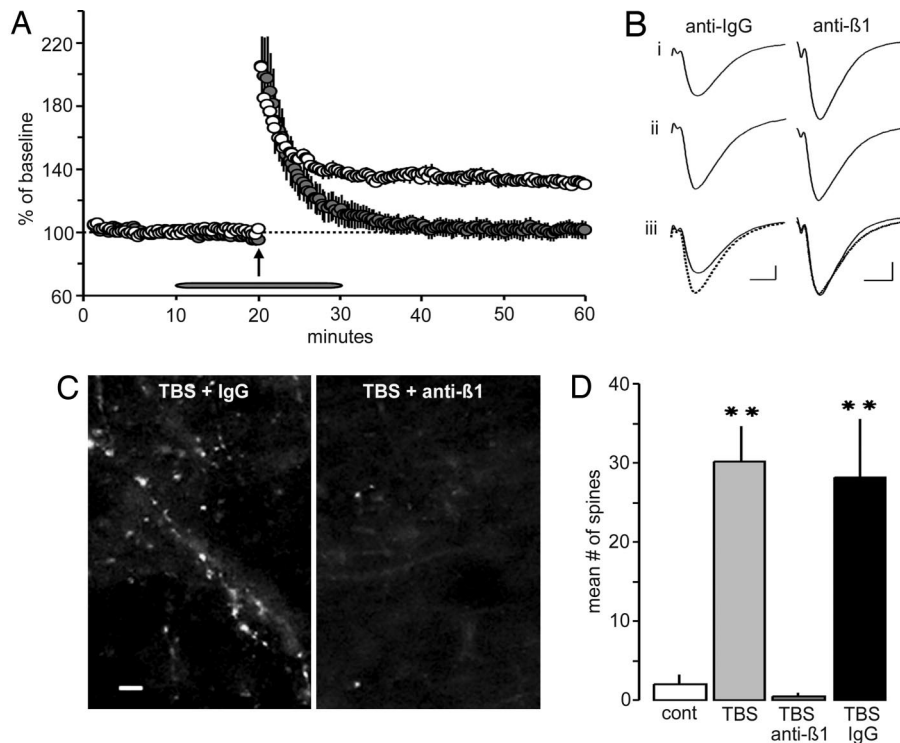
Fig. 4. Neutralizing antibodies against β1 integrins blocks actin polymerization and LTP consolidation. (*A*) Topical application of neutralizing β1 antisera (filled circles) did not affect baseline fEPSPs (−2 ± 5.8%) or initial potentiation after TBS (arrow) but completely disrupted consolidation (% potentiation at 30 min: 1 ± 13%; n = 6). Control IgG (open circles) had no effect (% potentiation at 30 min: 40 ± 10.8%; n = 5). (*B*) The same β1 antisera did not disturb the baseline fEPSP waveform (*i*); LTP was intact in the presence of control IgG but not in slices treated with anti-β1 (*ii* and *iii*). (Calibration, 0.5 mV, 5 msec.) (*C*) Spine labeling appeared normal after TBS in slices treated with control IgG but was virtually absent in those treated with anti-β1. (Scale bar, 5 μm.) (*D*) The number of phalloidin-positive spines was approximately the same in slices receiving TBS in the presence of anti-β1 (2.0 ± 1.1 per 550 μm²) and in slices receiving baseline stimulation (5 ± 5.7 per 550 μm²). Conversely, the mean value for control IgG-plus-TBS cases (26 ± 5.9 per 550 μm²) was 10-fold greater than for slices receiving baseline stimulation (**, P < 0.001).

chamber perfused with preheated artificial cerebrospinal fluid (ACSF) containing 124 mM NaCl, 3 mM KCl, 1.25 mM KH_2PO_4, 3.4 mM $CaCl_2$, 2.5 mM $MgSO_4$, 26 mM $NaHCO_3$, and 10 mM D-glucose (pH 7.35). Unless otherwise noted, chemicals were purchased from Sigma. Slices were continuously perfused with ACSF at 1.75–2 ml/min (31 ± 1°C) with the slice surface exposed to warm, humidified 95% O_2/5% CO_2. Application of rhodamine-phalloidin (6 μM) began after a 1.5-h incubation. Field excitatory postsynaptic potentials (fEPSPs) were recorded from CA1b stratum radiatum by using a single glass pipette (2–3 MΩ). Orthodromic stimulation was delivered at two sites (CA1a and CA1c) in the apical Schaffer collateral-commissural projections to provide convergent activation of CA1b pyramidal cells. Pulses were administered in an alternating fashion to the two electrodes at 0.05 Hz by using a current that elicited a 50% maximal response. Rhodamine-phalloidin was applied topically from a micropipette every 5 min for 20 min. After this procedure, baseline recordings were collected for 5 min and then 2, 5, or 10 theta bursts (each containing four pulses at 100 Hz, with an interburst interval of 200 ms) were delivered to one of the stimulation electrodes. This step was repeated 2 min later to the second electrode; slices were collected 15 min after the second stimulation episode. Slices in the control group received baseline stimulation for 15 min after rhodamine-phalloidin treatment. In some experiments, theta-pulse stimulation (three 1-min trains of single pulses delivered at 5 Hz, with an intertrain interval of 1 min) was applied 30 sec, 2 min, or 30 min after inducing LTP. Recordings were continued for an additional 15 min. Electrophysiological data were collected and digitized by using the NAC 2.0 neurodata acquisition system (Theta Burst, Irvine, CA) and

stored on a disk. Immediately after the testing period, slices were fixed in 4% paraformaldehyde in 0.1 M phosphate buffer (pH 7.4).

Drug Application. For some electrophysiological studies, function-blocking antisera to β1 integrin (MAB1987Z from Chemicon International, Temecula, CA, and #555002 from BD Biosciences, San Diego) or control anti-mouse Ig (IgG) (#PP100 from Chemicon) were diluted to a working pipette concentration of 0.2 mg/ml in ACSF immediately before use. The β1 antisera used have been shown to block integrin ligand effects on synaptic kinase signaling and N-methyl-D-aspartate receptor-mediated excitatory postsynaptic currents (EPSCs) in rat hippocampal slices (MAB1987Z) (50) and on intracellular calcium levels in rat cortical neurons (MAB1987Z and #555002) (C.M.G., unpublished observations). Sera were locally applied as described in ref. 14. Infusions began 10 min before TBS and continued for 10 min after TBS. In separate experiments designed to visualize the effects of antisera on F-actin, the anti-β1 or control-IgG was diluted to 0.2 mg/ml in 6 μM rhodamine-phalloidin and then topically applied. In experiments testing adenosine effects on F-actin, adenosine was diluted to a working concentration of 200 μM in ACSF before testing. Bath infusions of adenosine began 3 min before TBS so that it reached the slice immediately after induction of LTP.

Intracellular Application of Rhodamine-Phalloidin. Hippocampal slices were prepared (as described above), placed in a holding chamber for 2 h, and then transferred to a recording chamber; throughout, slices were submerged in ACSF oxygenated with

95% O_2/5% CO_2. In the recording chamber, ACSF was infused at 1.2 ml/min, and experiments were carried out at 32°C. CA1 pyramidal neurons were visualized by using an infrared microscope (BX50WI; Olympus, Melville, NY) and differential interference contrast microscopy configuration. Whole-cell recordings were made with 3–5 MΩ recording pipettes containing 130 mM Cs gluconate, 10 mM CsCl, 0.2 mM EGTA, 8 mM NaCl, 2 mM ATP, 0.3 mM GTP, and 10 mM Hepes (pH 7.35) (290–300 mosM). As described in ref. 7, previous studies determined that 6 μM rhodamine-phalloidin within the pipette does not interfere with baseline physiology or LTP induction. Holding potentials were set to −70 mV after correcting for the junction potential. Excitatory postsynaptic currents were recorded with a patch amplifier (Axopatch-1D; Axon Instruments, Burlingame, CA) with a four-pole low-pass Bessel filter at 2 kHz and digitized at 10 kHz. Two bipolar stimulating electrodes were placed in stratum radiatum, one on each side of the recording site. Baseline and post-theta-burst recording periods were performed as described by Lin *et al.* (7). Baseline responses were collected for 30 min, after which either two or five theta bursts were applied through one of the two stimulation electrodes. Holding potentials were reduced to 0 mV when TBS was applied and switched back to −70 mV afterward. Slices were fixed in 4% paraformaldehyde 30 min after TBS.

Imaging and Measurements. After 12–16 h in 4% paraformaldehyde, slices were cryoprotected in 20% sucrose/phosphate buffer, sectioned (freezing microtome, 25 μM) parallel to the broad slice surface, slide-mounted, and coverslipped with VECTASHIELD (Vector Laboratories). Rhodamine-phalloidin labeling was examined under epifluoresence illumination by using a Zeiss Axioscop microscope equipped with an AxioCam camera and AXIOVISION 3.1 software. The wavelength used for rhodamine-phalloidin imaging was 543 nm.

Labeled spines and dendritic segments were measured and counted as described in ref. 7. Final confirmation of accurate spine counts was achieved by hand, using original images to verify that target structures had been correctly identified.

1. Ribot, T. (1882) *Diseases of Memory* (Appleton, New York).
2. Duncan, C. P. (1948) *J. Comp. Physiol. Psychol.* **42,** 32–44.
3. Gall, C. M. & Lynch, G. (2005) in *Synaptic Plasticity and Transsynaptic Signaling*, eds. Stanton, P. K., Bramham, C. & Scharfman, H. E. (Springer, New York), pp. 469–494.
4. McGaugh, J. L. (2000) *Science* **287,** 248–251.
5. Bailey, C. H., Bartsch, D. & Kandel, E. R. (1996) *Proc. Natl. Acad. Sci. USA* **93,** 13445–13452.
6. Davis, H. P. & Squire, L. R. (1984) *J. Neurobiol.* **96,** 518–559.
7. Lin, B., Kramár, E. A., Bi, X., Brucher, F. A., Gall, C. M. & Lynch, G. (2005) *J. Neurosci.* **25,** 2062–2069.
8. Matynia, A., Kushner, S. A. & Silva, A. J. (2002) *Annu. Rev. Genet.* **36,** 687–720.
9. Fonseca, R., Nagerl, U. V., Morris, R. G. & Bonhoeffer, T. (2004) *Neuron* **44,** 1011–1020.
10. Barrionuevo, G., Schottler, S. & Lynch, G. (1980) *Life Sci.* **27,** 2385–2391.
11. Staubli, U. & Chun, D. (1996) *J. Neurosci.* **16,** 853–860.
12. DeMali, K. A., Wennerberg, K. & Burridge, K. (2003) *Curr. Opin. Cell Biol.* **15,** 572–582.
13. Chan, C.-S., Weeber, E. J., Kurup, S., Sweatt, J. D. & Davis, R. L. (2003) *J. Neurosci.* **23,** 7107–7116.
14. Kramár, E. A., Bernard, J. A., Gall, C. M. & Lynch, G. (2002) *Neuroscience* **110,** 29–39.
15. Chun, D., Gall, C. M., Bi, X. & Lynch, G. (2001) *Neuroscience* **105,** 815–829.
16. Staubli, U. & Lynch, G. (1990) *Brain Res.* **513,** 113–118.
17. Staubli, U., Chun, D. & Lynch, G. (1998) *J. Neurosci.* **18,** 3460–3469.
18. Huang, Y.-Q., Lu, W. Y., Ali, D. W., Pelkey, K. A., Pitcher, G. M., Lu, Y. M., Aoto, H., Roder, J. C., Saski, T., Salter, M. W. & MacDonald, J. F. (2001) *Neuron* **29,** 485–496.
19. Yang, Y. C., Ma, Y. L., Chen, S. K., Wang, C. W. & Lee, E. H. Y. (2003) *J. Neurosci.* **23,** 4072–4080.
20. Larson, J., Xiao, P. & Lynch, G. (1993) *Brain Res.* **600,** 97–102.
21. Burette, F., Jay, T. M. & Saroche, S. (1997) *J. Neurophysiol.* **78,** 1155–1160.
22. Huang, C. C., Liang, Y. C. & Hsu, K. S. (2001) *J. Biol. Chem.* **276,** 48108–48117.
23. Arai, A., Kessler, M. & Lynch, G. (1990) *Neurosci. Lett.* **119,** 41–44.
24. Pinkstaff, J. K., Detterich, J., Lynch, G. & Gall, C. M. (1999) *J. Neurosci.* **19,** 1514–1556.
25. Ridley, A. J., Schwartz, M. A., Burridge, K., Firtel, R. A., Ginsberg, M. H., Borisy, G., Parsons, J. T. & Horwitz, A. F. (2003) *Science* **302,** 1704–1709.
26. Lee, K., Schottler, F., Oliver, M. & Lynch, G. (1980) *J. Neurophysiol.* **44,** 247–258.
27. Matsuzaki, M., Honkura, N., Ellis-Davies, G. C. & Kasai, H. (2004) *Nature* **429,** 761–766.
28. Yuste, R. & Bonhoeffer, T. (2001) *Annu. Rev. Neurosci.* **24,** 1071–1089.
29. Staubli, U. & Lynch, G. (1987) *Brain Res.* **435,** 227–234.
30. Abraham, W. C., Logan, B., Greenwood, J. M. & Dragunow, M. (2002) *J. Neurosci.* **22,** 9626–9634.
31. Staubli, U., Vanderklish, P. W. & Lynch, G. (1990) *Behav. Neural Biol.* **53,** 1–5.
32. Krucker, T., Siggins, G. R. & Halpain, S. (2000) *Proc. Natl. Acad. Sci. USA* **97,** 6856–6861.
33. Fukazawa, Y., Saitoh, Y., Ozawa, F., Ohta, Y., Mizuno, K. & Inokuchi, K. (2003) *Neuron* **38,** 447–460.
34. Ackermann, M. & Matus, A. (2003) *Nat. Neurosci.* **6,** 1194–1200.
35. Fischer, M., Kaech, S., Knutti, D. & Matus, A. (1998) *Neuron* **20,** 847–854.
36. Okamoto, K.-I., Nagai, T., Miyawaki, A. & Hayashi, Y. (2004) *Nat. Neurosci.* **7,** 1104–1112.
37. Kramár, E. A. & Lynch, G. (2003) *Neuroscience* **118,** 387–398.
38. Hartwig, J. H. (1992) *J. Cell Biol.* **118,** 1421–1442.
39. Ma, L., Rohatgi, R. & Kirschner, M. W. (1998) *Proc. Natl. Acad. Sci. USA* **95,** 15362–15367.
40. Vanderklish, P. W., Krushel, L. A., Holst, B. H., Gally, J. A., Crossin, K. L. & Edelman, G. M. (2000) *Proc. Natl. Acad. Sci. USA* **97,** 2253–2258.
41. Matsuoka, Y., Li, X. & Bennett, V. (1998) *J. Cell Biol.* **42,** 485–497.
42. Nakagawa, T., Engler, J. A. & Sheng, M. (2004) *Neuropharmacology* **47,** 734–745.
43. Tomimatsu, Y., Idemoto, S., Moriguchi, S., Watanabe, S. & Nakanishi, H. (2002) *Life Sci.* **72,** 355–361.
44. Lynch, G. & Baudry, M. (1988) *Science* **224,** 1057–1063.
45. del Cerro, S., Larson, J., Oliver, M. & Lynch, G. (1990) *Brain Res.* **530,** 91–95.
46. Vanderklish, P., Saido, T. C., Gall, C., Arai, A. & Lynch, G. (1995) *Mol. Brain Res.* **32,** 25–35.
47. Stafstrom-Davis, C. A., Ouimet, C. C., Feng, J., Allen, P. B., Greengard, P. & Houpt, T. A. (2001) *Learn. Mem.* **8,** 272–278.
48. Dash, P. K., Orsi, S. A., Moody, M. & Moore, A. N. (2004) *Biochem. Biophys. Res. Commun.* **322,** 893–898.
49. Lamprecht, R., Farb, C. R. & LeDoux, J. E. (2002) *Neuron* **36,** 727–738.
50. Bernard-Trifilo, J. A., Kramár, E. A., Torp, R., Lin, C.-Y., Pineda, E. A., Lynch, G. & Gall, C. M. (2005) *J. Neurochem.* **93,** 834–849.